

OTFusion: Bridging Vision-only and Vision-Language Models via Optimal Transport for Transductive Zero-Shot Learning

Qiyu Xu, Wenyang Chen, Zhanxuan Hu, Huaifeng Li, Yonghang Tai

Abstract

Transductive zero-shot learning (ZSL) aims to classify unseen categories by leveraging both semantic class descriptions and the distribution of unlabeled test data. While Vision-Language Models (VLMs) such as CLIP excel at aligning visual inputs with textual semantics, they often rely too heavily on class-level priors and fail to capture fine-grained visual cues. In contrast, Vision-only Foundation Models (VFMs) like DINOv2 provide rich perceptual features but lack semantic alignment. To exploit the complementary strengths of these models, we propose *OTFusion*, a simple yet effective training-free framework that bridges VLMs and VFMs via *Optimal Transport*. Specifically, *OTFusion* aims to learn a shared probabilistic representation that aligns visual and semantic information by minimizing the transport cost between their respective distributions. This unified distribution enables coherent class predictions that are both semantically meaningful and visually grounded. Extensive experiments on 11 benchmark datasets demonstrate that *OTFusion* consistently outperforms the original CLIP model, achieving an average accuracy improvement of nearly 10%, all without any fine-tuning or additional annotations. The code will be publicly released after the paper is accepted.

Introduction

Zero-shot learning (ZSL) has emerged as a promising paradigm for recognizing novel categories without requiring labeled examples (Lampert, Nickisch, and Harmeling 2009; Han et al. 2021). In particular, *Transductive ZSL*, where the entire unlabeled test set is available at inference time, offers a valuable opportunity to exploit the global data distribution for more accurate predictions (Wang et al. 2023; Fu et al. 2015). Recent progress in this area has been largely driven by Vision-Language Models (VLMs), such as CLIP (Radford et al. 2021), which align images and textual labels within a joint embedding space. By encoding class names into textual prompts and comparing them with image features, these models enable direct zero-shot classification (Martin et al. 2024; Zanella, Gérin, and Ayed 2024).

Despite their impressive generalization capability, VLMs often struggle to associate text semantics with precise visual regions due to their image-level alignment training.

This limitation leads to an over-reliance on semantic priors and degraded performance under domain shifts or in tasks requiring fine-grained distinctions. In contrast, Vision-only Foundation Models (VFMs) such as DINOv2 (Oquab et al. 2023), trained with self-supervised objectives, excel at capturing rich visual patterns and perform strongly across various downstream tasks (Zhang and Tan 2025). However, VFMs lack inherent connections to class semantics, rendering them unsuitable for zero-shot classification without additional adaptation.

To further investigate this gap, we visualize three spaces using t-SNE: the visual spaces of CLIP’s vision encoder and DINOv2, and the probabilistic space of CLIP. As illustrated in Figure 1, CLIP’s visual features exhibit only coarse semantic structures with considerable category overlap. In contrast, DINOv2 features form tight, well-separated clusters, indicating significantly stronger visual discrimination. More importantly, the spatial distribution of DINOv2 features and the semantic layout of CLIP show clear structural complementarity. This observation suggests that VFMs provide highly discriminative visual priors that can enhance the semantic capabilities of VLMs. Naturally, this raises question: *Can we effectively combine the strengths of both model families to improve zero-shot classification performance?* A recent effort in this direction is DINO-assisted prompt learning (Imam et al. 2024), which leverages a DINO-based labeling network to guide prompt tuning of the vision encoder in VLMs. While this approach yields strong performance, it requires substantial computational resources and struggles to generalize across different foundation models.

In this work, we propose *OTFusion*, a simple yet effective training-free framework that bridges VFMs and VLMs through the lens of *Optimal Transport* (Villani et al. 2008; Cuturi 2013). Rather than forcing the two model types into a shared embedding space, we treat each model as inducing a probability distribution over class labels. *OTFusion* then constructs a unified probabilistic representation by minimizing the transport cost between these distributions, enabling predictions that are both semantically meaningful and visually grounded, as shown in Figure 1. Crucially, *OTFusion* operates entirely in the probability space, which allows for flexible integration of diverse models, including multiple VLMs and VFMs. In addition, *OTFusion* is highly compatible with a wide range of training-based methods that

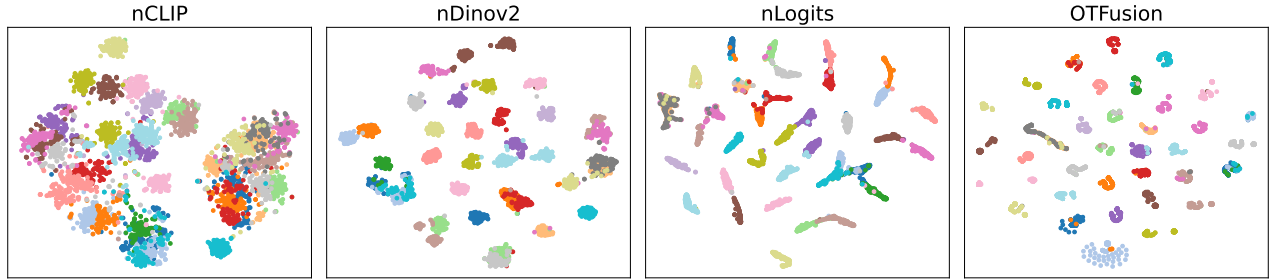


Figure 1: t-SNE visualization of predicted clusters on the `Pets` dataset. *OTFusion* significantly improves cluster compactness and separation over CLIP, highlighting superior integration of visual and semantic cues.

rely on pseudo-labels, such as Lafter (Mirza et al. 2023) and CPL (Zhang et al. 2024a). Specifically, *OTFusion* can serve as a plug-and-play component to generate more reliable soft pseudo-labels or enhance existing ones by integrating complementary knowledge from multiple foundation models. We evaluate our method across 11 standard zero-shot benchmarks, and demonstrate that *OTFusion* consistently outperforms the original CLIP model, achieving an average accuracy improvement of nearly 10%. Our approach is lightweight, scalable, and fully training-free, making it well-suited for deployment in low-resource scenarios.

Contributions. The main contributions of this paper are summarized as follows:

- *Novel perspective.* To the best of our knowledge, this is the first work that systematically investigates the complementary strengths of VFMs and VLMs in the *Transductive* ZSL setting, opening up a new direction for enhancing zero-shot performance.
- *Novel method.* We introduce *OTFusion*, a simple yet effective *training-free* framework that unifies predictions from VLMs and VFMs via Optimal Transport. Unlike traditional ensemble or Mixture of Experts approaches, *OTFusion* models each foundation model as a probability distribution over class labels and constructs a shared probabilistic representation by minimizing transport cost, enabling semantically coherent and visually grounded predictions.
- *Promising results.* Extensive experiments on 11 widely-used zero-shot benchmarks demonstrate that *OTFusion* consistently improves CLIP, achieving an average accuracy gain of 10%, all without any fine-tuning or additional annotations. These results highlight its practical utility for scalable deployment in resource-constrained scenarios.

Related Work

Zero-shot Learning

Zero-shot learning (ZSL) aims to recognize unseen classes by transferring semantic knowledge from seen categories through visual-semantic interactions (Liu et al. 2023). Existing methods can be broadly categorized into *Inductive* and *Transductive* paradigms.

Inductive ZSL. *Inductive* ZSL assumes no access to test-time data during training or adaptation. Traditional approaches typically follow two main directions: *embedding-based methods* (Chen et al. 2022, 2024; Hou et al. 2025), which learn a joint space to compare image and class semantics; and *generative methods* (Hou et al. 2024; Chen et al. 2023; Hou et al. 2025), which synthesize visual features for unseen classes via conditional generative models. Recently, large-scale VLMs such as CLIP (Radford et al. 2021) have significantly advanced ZSL. These models are pre-trained on massive image-text pairs to align visual and linguistic representations via contrastive learning. During inference, class names are converted into textual prompts, and classification is achieved by measuring similarity between image embeddings and those of the prompts, eliminating the need for hand-crafted attributes.

Despite their impressive generalization to novel categories, VLMs often over-rely on global semantic cues and underperform in scenarios requiring fine-grained discrimination or robustness to domain shift. To mitigate these issues, recent works focus on refining distance metrics (Guo et al. 2023; Zhou et al. 2023), improving prompt design (Roth et al. 2023; Novack et al. 2023), or augmenting with synthetic samples (Udandarao, Gupta, and Albanie 2023; Zhang et al. 2023). Nonetheless, most of these methods also operate under the inductive setting, without leveraging the unlabeled test distribution.

Transductive ZSL. *Transductive* ZSL assumes the availability of the entire unlabeled test set at inference time, which allows leveraging the test distribution to improve prediction accuracy. Various techniques have been proposed under this setting, including label propagation (Kalantidis, Tolias et al. 2024; Li et al. 2025), distribution alignment (Martin et al. 2024; Zanella, Gérin, and Ayed 2024), and test-time adaptation (Hu et al. 2024; Qian, Xu, and Hu 2023; Zhang et al. 2024b; Mirza et al. 2023; Khattak et al. 2025). These methods aim to reduce semantic shift and uncover the latent structure of test instances. While *Transductive* ZSL approaches show clear advantages, few works have explored how to integrate knowledge from diverse foundation models during inference. A recent effort in this direction is DINO-assisted prompt learning (Imam et al. 2024), which leverages a DINO-based labeling network to guide prompt tuning of the vision encoder in VLMs. While this approach yields

strong performance, it requires substantial computational resources and struggles to generalize across different foundation models. Our work addresses this gap by proposing a model-agnostic fusion mechanism that operates solely in the label probability space.

Mixture of Experts

Our framework is also conceptually related to Mixture of Experts (MoE) (Shazeer et al. 2017; Kar et al. 2024; Li et al. 2024; Azadani et al. 2025), which aims to improve generalization by combining the outputs of multiple expert models. However, conventional MoE systems typically rely on a learned gating mechanism and require joint training of all expert components, making them less suitable for zero-shot or low-resource settings. In contrast, *OTFusion* acts as a training-free and plug-and-play probabilistic mixture model, where each foundation model serves as an expert that defines a distribution over class labels. By leveraging *Optimal Transport* to align these distributions, *OTFusion* enables flexible fusion of an arbitrary number of VLMs and VFMs without additional training or architectural modification. This provides a scalable alternative to traditional MoE methods, particularly well-suited for *Transductive ZSL*.

Method

Preliminary

We consider the problem of *Transductive ZSL*, where we are given a set of unlabeled test images $\mathcal{X}_t = \{x_i\}_{i=1}^N$ and a set of class-level semantic descriptions $\mathcal{S} = \{s_j\}_{j=1}^C$ (e.g., textual names or attributes). The goal is to assign each image x_i a class label from the unseen classes based on semantic alignment and the underlying data distribution. Our method builds upon two types of pretrained foundation models: VFMs and VLMs. We briefly describe these two model families below.

VFMs VFMs are self-supervised vision encoders trained on large-scale unlabeled image datasets. They aim to learn transferable and high-quality representations without relying on labels. Among them, DINOv2 (Oquab et al. 2023) has shown state-of-the-art performance across many downstream tasks. Given an image x_i , the VFM encoder f_v outputs a visual embedding $\mathbf{v} = f_v(x_i) \in \mathbb{R}^d$. These embeddings are purely visual and do not encode semantic label information directly, but they often exhibit strong intra-class compactness and inter-class separability.

VLMs Unlike VFMs, VLMs are pretrained to align images and texts within a shared embedding space using large-scale image-text pairs. A representative example is CLIP (Radford et al. 2021), which jointly learns an image encoder f_I and a text encoder f_T through contrastive learning. Given an image x_i , the image encoder f_I produces a visual embedding $\mathbf{v}_i = f_I(x_i) \in \mathbb{R}^d$. At the same time, class names are formatted into textual prompts s_j (e.g., "a photo of a [class]") and encoded as semantic prototypes $\mathbf{t}_j = f_T(s_j)$. At inference time, VLMs support zero-shot

reasoning by comparing image embeddings with class prototypes, yielding a probability distribution over classes:

$$y_{ij} = \frac{\exp(\tau \cdot \cos(\mathbf{v}_i, \mathbf{t}_j))}{\sum_{k=1}^C \exp(\tau \cdot \cos(\mathbf{v}_i, \mathbf{t}_k))}, \quad (1)$$

where $\cos(\cdot, \cdot)$ denotes cosine similarity and τ is a temperature parameter. The resulting matrix $\mathbf{Y} \in \mathbb{R}^{N \times C}$ encodes class probabilities for all test data.

OTFusion: Bridging VFMs and VLMs via Optimal Transport

Our goal is to leverage the complementary strengths of VFMs and VLMs for *Transductive ZSL*. We propose a training-free framework, *OTFusion*, that fuses class probability distributions derived from both sources via *Optimal Transport*. The details are as follows.

Modeling Visual Distributions via Gaussian Mixture Model (GMM). Given test data $\mathcal{X} = \{x_1, \dots, x_N\}$, we extract visual features $\mathbf{v}_i = f_v(x_i)$ and fit a GMM on $\mathbf{V} \in \mathbb{R}^{N \times d}$. Specifically, the GMM assumes:

$$p(\mathbf{v}) = \sum_{c=1}^C \pi_c \cdot \mathcal{N}(\mathbf{z}; \mu_c, \Sigma_c), \quad (2)$$

where π_c are mixture weights and μ_c, Σ_c are component parameters. In practice, a shared diagonal covariance matrix Σ across all classes is typically adopted to reduce computational complexity (Zanella, Gérin, and Ayed 2024). Using a shared diagonal covariance Σ , we compute soft posteriors:

$$\mathbf{p}_i = [p(y=1|\mathbf{z}_i), \dots, p(y=C|\mathbf{z}_i)] \in \Delta^C, \quad (3)$$

where Δ^C denotes the C -dimensional probability simplex. Stacking yields the visual distribution matrix $\mathbf{P} \in \mathbb{R}^{N \times C}$.

Given multiple pre-trained VFMs $\{f_v^{(1)}, \dots, f_v^{(K)}\}$, a straightforward approach is to extract feature vectors $\mathbf{z}_i^{(k)} = f_v^{(k)}(x_i)$ for each model and concatenate them into a joint representation: $\mathbf{z}_i = [\mathbf{z}_i^{(1)}, \dots, \mathbf{z}_i^{(K)}]$. GMM fitting and inference can then be performed as before to obtain a richer visual distribution \mathbf{P} . However, this concatenation-based strategy incurs substantial computational and memory overhead as K increases, limiting its scalability in practice. To address this limitation, we further propose a more general and flexible framework that fuses the outputs of multiple foundation models in a principled manner via *Optimal Transport*, without requiring explicit feature concatenation.

Distribution Fusion via Optimal Transport. Our goal is to unify two complementary sources of class-discriminative information: the visual prior \mathbf{P} derived from VFMs and the semantic prior \mathbf{Y} derived from VLMs. To achieve this, we cast the distribution fusion process as an *Optimal Transport* problem. Intuitively, *Optimal Transport* seeks a soft alignment $\mathbf{Q} \in \mathbb{R}^{N \times K}$ between the N image samples and K classes, such that the transport plan \mathbf{Q} simultaneously respects the structure of the visual distribution \mathbf{P} and the semantic distribution \mathbf{Y} . Formally, the optimization objective of *OTFusion* is formulated as the following :

$$\mathcal{L}(\mathbf{Q}, \mu, \Sigma) = \max_{\mathbf{Q} \in \mathcal{Q}} \text{Tr}(\mathbf{Q}^\top \mathbf{P}) + \lambda \text{Tr}(\mathbf{Q}^\top \mathbf{Y}) + \epsilon \mathcal{H}(\mathbf{Q}), \quad (4)$$

where the first two terms promote alignment between \mathbf{Q} and the guidance distributions, and the third term introduces an entropy regularizer $\mathcal{H}(\mathbf{Q}) = -\sum_{ij} Q_{ij} \log Q_{ij}$ that encourages smoother and more stable transport plans. The hyperparameter λ balances the influence of semantic and visual information, and ϵ controls the entropy smoothness. We follow (Caron et al. 2020) and keep ϵ small to avoid overly uniform predictions. This formulation is subject to the transport polytope constraint:

$$\mathcal{Q} = \{\mathbf{Q} \in \mathbb{R}_+^{N \times K} \mid \mathbf{Q}\mathbf{1}_K = \mathbf{1}_N, \mathbf{Q}^\top \mathbf{1}_N = \mathbf{1}_K\}, \quad (5)$$

which ensures that \mathbf{Q} is a doubly stochastic matrix, effectively defining a soft assignment of each sample to all possible classes while maintaining global mass conservation.

Importantly, a key advantage of our joint objective in Eq. (4) is the mutual reinforcement between the learned prediction distribution \mathbf{Q} and the visual distribution \mathbf{P} . During optimization, \mathbf{Q} is jointly influenced by the GMM-induced visual assignment scores \mathbf{P} and the semantic distribution \mathbf{Y} from VLMs. In turn, the evolving \mathbf{Q} , which implicitly guides the update of GMM parameters (μ, Σ) , encouraging the formation of clusters that are not only visually coherent but also semantically meaningful. This bi-directional interaction prevents the GMM from collapsing into appearance-based, density-driven clusters that may ignore semantic structure, and instead facilitates the emergence of class boundaries that are both data-driven and semantically aligned.

Extension. Indeed, we can further generalize our framework to incorporate multiple VFMs and VLMs:

$$\begin{aligned} \mathcal{L}(\mathbf{Q}, \{\mu_i\}, \{\Sigma_i\}) = \max \sum_i \eta_i \text{Tr}(\mathbf{Q}^\top \mathbf{P}_i) \\ + \sum_i \lambda_i \text{Tr}(\mathbf{Q}^\top \mathbf{Y}_i) + \epsilon \mathcal{H}(\mathbf{Q}), \end{aligned} \quad (6)$$

where \mathbf{P}_i and \mathbf{Y}_i denote the class probability distributions obtained from the i -th VFM and VLM, respectively. The coefficients $\{\eta_i\}$ and $\{\lambda_i\}$ are balancing hyperparameters that control the contributions of each expert model. This formulation allows *OTFusion* to flexibly integrate information from a diverse set of foundation models in a unified optimization framework.

Optimization

Without loss of generality, we describe the optimization procedure for Eq. (6), which can be readily extended to the more general objective in Eq. (4). Our approach adopts an alternating optimization strategy between the prediction distribution \mathbf{Q} and the GMM parameters (μ, Σ) .

Initialization. We begin by initializing the soft visual assignment matrix $\mathbf{P}^{(0)}$ using the semantic distribution \mathbf{Y} predicted by the VLM. This semantically guided initialization provides a prior for estimating the initial GMM parameters $(\mu^{(0)}, \Sigma^{(0)})$ over the visual features \mathbf{X} , ensuring the GMM is initially aligned with the high-level semantic knowledge.

Algorithm 1: Training-free Optimization of *OTFusion*

Require: Visual features $\mathbf{V} = \{\mathbf{v}_i\}_{i=1}^N$, VLM probability distribution $\mathbf{Y} \in \mathbb{R}^{N \times K}$, number of iterations T
Ensure: Prediction distribution \mathbf{Q} and GMM parameters (μ, Σ)

- 1: Initialize $\mathbf{P}^{(0)}$ using \mathbf{Y} ; estimate $(\mu^{(0)}, \Sigma^{(0)})$
- 2: **for** $t = 1$ to T **do**
- 3: Compute probability distribution $\mathbf{P}^{(t)}$ via GMM E-step using $(\mu^{(t-1)}, \Sigma^{(t-1)})$;
- 4: Update probability distribution $\mathbf{Q}^{(t)}$ using Eq. (8);
- 5: Update $(\mu^{(t)}, \Sigma^{(t)})$ using Eq. (11) and Eq. (12)
- 6: Convergence check.
- 7: **end for**
- 8: **return** $\mathbf{Q}^*, (\mu^{(T)}, \Sigma^{(T)})$

Alternating Optimization. At iteration t , given the current GMM parameters $(\mu^{(t-1)}, \Sigma^{(t-1)})$, we compute the visual class distribution $\mathbf{P}^{(t)}$ using the E-step of the GMM. Subsequently, we update the prediction distribution $\mathbf{Q}^{(t)}$ by solving the following entropy-regularized Optimal Transport problem:

$$\max_{\mathbf{Q} \in \mathcal{Q}} \sum_i \eta_i \text{Tr}(\mathbf{Q}^\top \mathbf{P}_i) + \sum_i \lambda_i \text{Tr}(\mathbf{Q}^\top \mathbf{Y}_i) + \epsilon \mathcal{H}(\mathbf{Q}) \quad (7)$$

which can be efficiently solved via the Sinkhorn algorithm (Cuturi 2013). Specifically,

$$\mathbf{Q}^{(t)} = \text{Diag}(\mathbf{u}) \cdot \exp \left(\frac{\sum_i \eta_i \mathbf{P}_i^{(t)} + \sum_i \lambda_i \mathbf{Y}_i}{\epsilon} \right) \cdot \text{Diag}(\mathbf{v}), \quad (8)$$

where $\mathbf{u} \in \mathbb{R}^K$ and $\mathbf{v} \in \mathbb{R}^N$ are scaling vectors iteratively updated as:

$$\mathbf{u}^{(s+1)} = \frac{\mathbf{1}_K}{\mathbf{K} \mathbf{v}^{(s)}}, \quad (9)$$

$$\mathbf{v}^{(s+1)} = \frac{\mathbf{1}_N}{\mathbf{K}^\top \mathbf{u}^{(s+1)}}, \quad (10)$$

with $\mathbf{K} = \exp \left(\frac{\sum_i \eta_i \mathbf{P}_i^{(t)} + \sum_i \lambda_i \mathbf{Y}_i}{\epsilon} \right)$. In practice, a small number of iterations (e.g., 3) is sufficient for convergence. Obviously, Eq. (8) demonstrates that $\mathbf{Q}^{(t)}$ aligns with both the visual structure and semantic guidance.

Updating GMM Parameters via \mathbf{Q} . Rather than relying on \mathbf{P} as in traditional EM updates, we leverage the semantically enriched $\mathbf{Q}^{(t)}$ to refine the GMM parameters, thereby enforcing stronger semantic alignment. The updates are computed as:

$$\mu_k^{(t)} = \frac{\sum_i Q_{ik}^{(t)} \mathbf{v}_i}{\sum_i Q_{ik}^{(t)}}, \quad (11)$$

$$\Sigma^{(t)} = \frac{1}{N} \sum_i \sum_k Q_{ik}^{(t)} (\mathbf{v}_i - \mu_k^{(t)}) (\mathbf{v}_i - \mu_k^{(t)})^\top, \quad (12)$$

which ensures that the resulting clusters are not only visually coherent but also semantically meaningful, avoiding convergence to purely density-driven partitions. We alternate between the above optimization steps, updating the prediction distribution \mathbf{Q} and refining the GMM parameters (μ, Σ) , iteratively until convergence. The full optimization algorithm is summarized in Algorithm 1.

Experiments

Experimental Setup

Datasets. Building on prior work (Zanella, Gérin, and Ayed 2024; Zhou et al. 2022b), we conduct an extensive evaluation of OTFusion across 11 diverse datasets, including ImageNet (Jia Deng and Fei-Fei 2009), SUN397 (Jianxiong Xiao and Torralba 2010), Aircraft (Subhransu Maji and Vedaldi 2013), Eurosat (Patrick Helber and Borth 2019), StanfordCars (Jonathan Krause and Fei-Fei 2013), Food101 (Bossard, Guillaumin, and Gool 2014), Pets (MParkhi et al. 2012), Flowers102 (Nilsback and Zisserman 2008), Caltech101 (Fei-Fei, Fergus, and Perona 2004), DTD (Cimpoi et al. 2014), and UCF101 (Soomro, Zamir, and Shah 2012). These datasets encompass a broad spectrum of image classification, allowing us to comprehensively assess the robustness and generalization capability of our method across distinct domains.

Benchmarks. We evaluate our proposed method, OTFusion, against a comprehensive set of representative approaches for both zero-shot adaptation tasks. These competing methods can be broadly categorized based on whether they require additional training: training-based and training-free. The training-based category includes TPT (Manli et al. 2022), DiffTPT (Feng et al. 2023), and CoCoOp (Zhou et al. 2022a), which rely on task-specific optimization to adapt prompts or model parameters. In contrast, training-free methods operate without any finetuning and include CLIP (Radford et al. 2021), VisDesc (Menon and Vondrick 2023), CuPL (Pratt et al. 2023), Sus-X (Udandara, Gupta, and Albanie 2023), CALIP (Guo et al. 2023), TDA (Karmenov et al. 2024), DMN (Zhang et al. 2024b), TransCLIP (Zanella, Gérin, and Ayed 2024), and ECALP (Li et al. 2025).

Implementation details. Our framework is built upon open-source implementations of vision-language and vision foundation models. We use the CLIP ViT-B/16 and ResNet-50 models released by OpenAI as the primary semantic predictors, without any additional fine-tuning. For visual prior extraction, we adopt DINOv2 ViT-L/14, selected for its strong clustering properties. During inference, each image is processed using a single-view center crop (224×224) to reduce computational overhead. Class names are embedded using a fixed prompt template without manual prompt ensembling or optimization. The output distributions from the vision and language branches are fused via our proposed OTFusion. The temperature parameter ϵ to control the entropy smoothness is set to 0.01, the balance parameters λ is set to 0.8. To maintain simplicity while integrating multiple VFM models, we enforce uniformity in η across all models,

subject to the normalization constraint $\sum_i \eta_i = 1$. All models run in inference-only mode, and no gradient updates are performed. Experiments are conducted on an NVIDIA 4090 GPU with 24GB of memory.

Main results

To assess the effectiveness of our method, OTFusion, we evaluate it on a broad spectrum of visual recognition benchmarks in the Transductive zero-shot setting. Our comparisons span several state-of-the-art training-based (indicated with *) and training-free methods, utilizing two widely adopted pre-trained backbones: CLIP-ViT/B16 and ResNet-50. Table 1 presents a comparison between OTFusion and several state-of-the-art methods across eleven datasets, where ‘ Δ ’ denotes the performance improvements over the baseline model, CLIP. Among the compared methods, CoCoOp, TPT, and DiffTPT require prompt tuning to adapt to specific tasks, which introduces additional training overhead and limits generalization. In contrast, our method is entirely training-free yet outperforms these methods by over 10% on average across both CLIP-ViT/B16 and ResNet50 backbones. While DMN achieves slightly better performance than OTFusion on the Aircraft, it depends on dual memory modules and task-specific hyperparameters, leading to higher computational costs and limited scalability. Moreover, OTFusion surpasses DMN on nearly all other datasets. ECALP achieves competitive results on DTD, but its reliance on dynamic graph construction brings considerable computational complexity. Other recent methods like TransCLIP and TDA also show strong performance but still fall short of OTFusion, particularly on datasets requiring robust generalization (e.g., Eurosat, Flowers102). Earlier methods, such as CuPL, Sus-X, VisDesc, and CALIP, perform moderately across datasets, but none consistently approach the overall effectiveness of OTFusion.

Ablation Study

We conduct a comprehensive ablation study to verify the effectiveness of each component in our framework, as summarized in Table 2. Specifically, **Y-only** performs *Optimal Transport* solely based on the semantic probability distribution \mathbf{Y} output by the VLMs, without utilizing any visual information. **CLIP-only** models the distribution derived exclusively from CLIP’s visual features, without incorporating perspectives from other VFMs. **DINOv2-only** relies solely on the visual distribution from DINOv2 to assess the contribution of different visual models. **Concatenation** fuses multiple visual features by concatenating them into a single input for GMM, serving as the most straightforward fusion strategy. OTFusion jointly trains by integrating probability distributions from multiple visual models along with the semantic distribution \mathbf{Y} . Lastly, **No joint-learning** performs inference by directly combining different distributions during testing without joint training, aiming to evaluate the necessity of joint optimization.

Importance of fusing vision feature. A central design choice of our framework is the integration of multiple visual feature spaces. As shown in Table 2, **Y-only** leads

Datasets	ImageNet	SUN397	Aircraft	Eurosat	StanfordCars	Food101	Pets	Flowers102	Caltech101	DTD	UCF101	Average
<i>(a) Comparison with state-of-the-art Zero-shot methods using CLIP-ViT/B16</i>												
CLIP	66.73	65.63	23.22	50.42	66.11	82.86	86.92	66.99	93.55	45.04	65.16	64.78
CoCoOp* (CVPR'22)	71.02	66.89	22.29	39.23	64.90	83.97	90.46	70.85	93.79	45.45	68.44	65.21
TPT* (NeurIPS'22)	68.98	65.50	24.78	42.44	66.87	84.67	87.79	68.98	94.16	47.75	68.04	65.45
DiffTPT* (ICCV'23)	70.30	65.74	25.60	43.13	67.01	<u>87.23</u>	88.22	70.10	92.49	47.00	62.67	65.41
TDA(CVPR'24)	69.51	67.62	23.91	58.00	67.28	86.14	88.63	71.42	94.24	47.40	70.66	67.71
DMN(CVPR'24)	<u>72.25</u>	70.18	30.03	59.43	67.96	85.08	92.04	74.49	<u>95.38</u>	<u>55.85</u>	72.51	70.47
TransCLIP(NeurIPS'24)	70.30	68.90	26.90	<u>65.10</u>	<u>69.40</u>	87.10	<u>92.60</u>	<u>76.70</u>	92.70	49.50	74.40	70.33
ECALP(ICLR'25)	71.26	<u>70.35</u>	<u>29.49</u>	56.53	68.20	85.72	92.31	75.96	94.40	56.32	<u>75.44</u>	70.54
Ours	76.76	72.06	27.48	81.86	70.96	87.89	94.58	85.18	96.11	53.72	77.80	74.95
Δ	<u>+10.03</u>	<u>+6.43</u>	<u>+4.26</u>	<u>+31.44</u>	<u>+4.85</u>	<u>+5.03</u>	<u>+7.66</u>	<u>+18.19</u>	<u>+2.56</u>	<u>+8.68</u>	<u>+12.64</u>	<u>+10.17</u>
<i>(b) Comparison with state-of-the-art Zero-shot methods using Resnet50</i>												
CLIP	58.17	58.85	17.04	36.20	55.74	77.36	85.72	66.10	85.68	42.79	61.88	58.68
DiffTPT*(ICCV'23)	60.80	62.72	17.60	41.04	<u>60.71</u>	<u>79.21</u>	83.40	63.53	86.89	40.72	62.67	59.94
CuPL(ICCV'23)	61.45	62.55	19.59	38.38	57.28	76.94	84.84	65.44	89.29	48.64	58.97	60.31
Sus-X(ICCV'23)	61.84	62.95	19.47	45.57	57.27	77.58	85.34	67.72	89.53	50.59	61.54	61.76
VisDesc(ICLR'23)	59.68	59.84	16.26	37.60	54.76	76.80	82.39	65.37	88.11	41.96	58.47	61.76
CALIP(ICCV'23)	60.57	58.59	17.76	38.90	56.27	77.42	86.21	66.38	87.71	42.39	61.72	64.00
TDA(CVPR'24)	61.35	62.53	17.61	42.11	57.78	77.75	86.18	68.74	89.70	43.74	64.18	61.06
DMN(CVPR'24)	<u>63.87</u>	64.39	22.77	48.72	60.02	76.70	86.78	67.93	<u>90.14</u>	50.41	65.34	63.37
TransCLIP(NeurIPS'24)	60.79	64.23	16.53	<u>59.64</u>	58.03	77.96	<u>89.53</u>	<u>72.15</u>	88.68	47.81	68.86	64.02
ECALP(ICLR'25)	62.64	<u>64.97</u>	<u>21.12</u>	49.09	60.56	76.97	88.20	69.39	89.94	54.49	66.67	<u>64.00</u>
Ours	73.77	69.37	18.45	74.41	64.64	82.54	93.84	75.07	95.29	<u>51.54</u>	76.05	70.45
Δ	<u>+15.60</u>	<u>+10.52</u>	<u>+1.41</u>	<u>+38.21</u>	<u>+8.90</u>	<u>+5.18</u>	<u>+8.12</u>	<u>+8.97</u>	<u>+9.61</u>	<u>+8.75</u>	<u>+14.17</u>	<u>+11.77</u>

Table 1: Comparison with several state-of-the-art methods on eleven datasets. The best results are highlighted in **bold**, and the second best results are highlighted in underline. * indicates that this method is training-based, otherwise it is not.

	ImageNet	SUN397	Aircraft	Eurosat	StanfordCars	Food101	Pets	Flowers102	Caltech101	DTD	UCF101	Average
native CLIP	66.60	62.50	24.70	48.30	65.60	85.90	89.10	70.70	93.20	43.50	67.50	65.24
<i>OTFusion</i>	76.76 <u>+10.16</u>	72.06 <u>+9.56</u>	27.48 <u>+2.78</u>	81.86 <u>+33.56</u>	70.96 <u>+5.36</u>	87.89 <u>+1.99</u>	94.58 <u>+5.48</u>	85.18 <u>+14.48</u>	96.11 <u>+2.91</u>	53.72 <u>+10.22</u>	77.80 <u>+10.30</u>	74.95 <u>+9.71</u>
Y-only	67.10 <u>+0.50</u>	63.39 <u>+0.89</u>	25.32 <u>+0.62</u>	50.47 <u>+2.17</u>	66.11 <u>+0.51</u>	85.95 <u>+0.05</u>	89.23 <u>+0.13</u>	70.97 <u>+0.27</u>	92.98 <u>-0.22</u>	44.80 <u>+1.30</u>	68.07 <u>+0.57</u>	65.85 <u>+0.61</u>
CLIP-only	69.90 <u>+3.30</u>	68.91 <u>+6.41</u>	26.07 <u>+1.37</u>	65.78 <u>+17.48</u>	69.72 <u>+4.12</u>	87.03 <u>+1.13</u>	92.56 <u>+3.46</u>	78.60 <u>+7.90</u>	94.12 <u>+0.92</u>	50.83 <u>+7.33</u>	77.08 <u>+9.58</u>	70.96 <u>+5.72</u>
Dinov2-only	76.71 <u>+10.11</u>	69.92 <u>+7.42</u>	27.45 <u>+2.75</u>	76.85 <u>+28.55</u>	71.62 <u>+6.02</u>	86.00 <u>+0.10</u>	94.22 <u>+5.12</u>	86.16 <u>+15.46</u>	97.04 <u>+3.84</u>	53.66 <u>+10.16</u>	76.58 <u>+9.08</u>	74.20 <u>+8.96</u>
Concatenation	77.14 <u>+10.54</u>	71.57 <u>+9.07</u>	28.86 <u>+4.16</u>	82.28 <u>+33.98</u>	72.14 <u>+6.54</u>	87.50 <u>+1.60</u>	94.82 <u>+5.72</u>	85.79 <u>+15.09</u>	96.84 <u>+3.64</u>	55.20 <u>+11.70</u>	78.80 <u>+11.30</u>	75.54 <u>+10.30</u>
No joint-learning	75.06 <u>+8.46</u>	68.60 <u>+6.10</u>	22.86 <u>-1.84</u>	71.31 <u>+23.01</u>	64.84 <u>-0.76</u>	86.80 <u>+0.90</u>	93.51 <u>+4.41</u>	83.43 <u>+12.73</u>	95.01 <u>+1.81</u>	52.07 <u>+8.57</u>	74.91 <u>+7.41</u>	71.67 <u>+6.43</u>

Table 2: Ablation study across 11 downstream datasets. We evaluate the contributions of different components in *OTFusion*, including distribution sources (**Y-only**, **CLIP-only**, **DINOv2-only**), fusion strategies (concatenation, distribution fusion), and training settings (with or without joint learning). *OTFusion* achieves consistent improvements over the CLIP baseline.

to only marginal gains over native CLIP (+0.61%), suggesting that weak supervisory signals are insufficient unless supported by discriminative features. In contrast, integrating vision features significantly improves zero-shot classification accuracy. Compared to using native CLIP (65.24%), both **CLIP-only** (70.96%) and **DINOv2-only** (74.20%) achieve substantial gains. Besides, when combining both visual sources via Feature concatenation or **Distribution Fusion** (used in *OTFusion*), performance further improves to 75.54% and 74.95%, respectively. This clearly indicates that multi-view visual features provide complementary information and jointly enhance the model’s performance.

Fusion Strategy Matters. Given the importance of integrating features, the method of fusion plays a key role. As shown in Table 2, naive concatenation of features performs well (75.54%), but our probabilistic fusion method, based on combining prediction distributions rather than raw features, achieves comparable or better results. This suggests

that both approaches are effective, and distribution-based fusion is advantageous due to its scalability and compatibility with probabilistic modeling.

Importance of Joint-learning. Our method leverages a joint optimization objective (Eq. (4)) that tightly couples the evolving prediction distribution \mathbf{Q} with both the visual assignments \mathbf{P} (from GMM) and the semantic prior \mathbf{Y} (from VLMs). The ablation result in Table 2 validates this effect: when joint learning is disabled (*No joint-learning*), the average accuracy drops significantly from 74.95% to 71.67%, with particularly large decreases observed on datasets like StanfordCars (6.12%), SUN397 (3.46%), and Eurosat (10.55%). These performance gaps underscore that decoupling the fusion module from the downstream prediction task weakens semantic alignment, leading to suboptimal clusters and degraded classification accuracy. In contrast, the joint-learning paradigm enables mutual reinforcement: the GMM’s clustering process is no

longer guided solely by visual similarity, but also influenced by the semantic structure induced by VLMs. Conversely, the predictive distribution \mathbf{Q} benefits from the refined visual clusters shaped by GMM, which evolve in tandem during learning.

Further Analyses

Parameter Sensitivity Analysis. We conduct a thorough sensitivity analysis on two key hyperparameters in our framework: the entropy regularization parameter ϵ in Optimal Transport, and the fusion coefficient λ in our distribution integration.

As shown in Figure 2, the left panel evaluates the impact of varying ϵ in the range $[10^{-3}, 10^{-1}]$. Across all 11 datasets, the performance remains remarkably stable, with only minimal fluctuations. This demonstrates that our method is largely insensitive to the choice of ϵ , and that a broad range of values can yield satisfactory results. Notably, overly large ϵ (e.g., 10^{-1}) may slightly degrade performance on certain datasets like Caltech101 and Food101. We recommend using $\epsilon = 0.01$ as a stable and effective default.

Besides, we also explore the influence of λ , which balances the contributions of the visual distribution from VFMs and the semantic distribution from VLMs. We vary λ between 0.1 and 1.0. As shown in Figure 2, *OTFusion* performs consistently well across different datasets when λ is relatively small (e.g., 0.1 to 0.7), demonstrating strong robustness and effective fusion between different foundation models. However, as λ increases beyond 0.7, we observe a performance drop on several datasets such as EuroSAT and Flowers12. This suggests that overemphasizing the semantic signal from \mathbf{Y} may lead to overfitting to potentially noisy pseudo-labels, thereby diminishing the contribution of discriminative visual patterns.

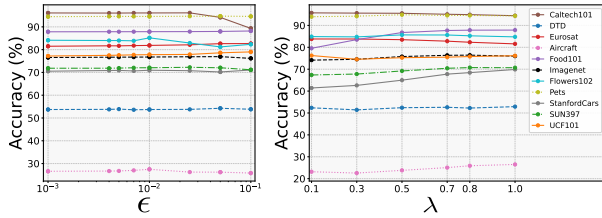


Figure 2: Parameter sensitivity analysis on ϵ (left) and λ (right) across 11 datasets. Performance remains stable over a wide range of values, highlighting the robustness of our proposed method *OTFusion*.

Convergence Analysis. We conduct convergence analysis by jointly examining the evolution of classification accuracy and optimization loss over training iterations, as shown in Figure 3. Each curve corresponds to a different dataset, reflecting the stability and learning dynamics of our model across diverse domains. From the left panel (Accuracy vs. Iteration), we observe that most datasets experience a sharp accuracy increase in the first few iterations, with performance typically plateauing after 5 rounds. Datasets such

as Caltech101 and Pets rapidly converge to high accuracies above 90%, demonstrating the model’s efficiency on structured visual domains. In contrast, more challenging datasets like Eurosat and DTD require a higher number of iterations.

Simultaneously, the right panel (Loss vs. Iteration) reveals that the overall loss increases rapidly at the early stage, due to the dynamic re-alignment between pseudo-labels and evolving visual clusters, but quickly stabilizes, typically within 3 to 5 iterations. This behavior confirms that our joint optimization effectively reaches equilibrium between the visual GMM model and the semantic guidance. Overall, *OTFusion* converges quickly and stably, balancing semantic alignment and visual clustering, and delivering consistent performance improvements with minimal training overhead.

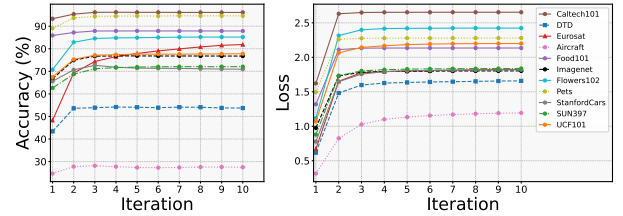


Figure 3: Convergence curves on 11 datasets. Left: Accuracy vs. Iteration. Right: Loss vs. Iteration. The method converges within a few iterations, demonstrating efficient and stable optimization.

Conclusion

In this paper, we proposed *OTFusion*, a flexible and training-free framework for Transductive ZSL. Our method leverages multiple pretrained foundation models by constructing visual distributions via Gaussian Mixture Models and semantic distributions from VLM predictions, and aligns them through an entropy-regularized optimal transport strategy where prediction distributions not only benefit from both visual and semantic cues, but also supervise the refinement of visual clusters. Extensive experiments across multiple benchmarks demonstrate the effectiveness and generality of *OTFusion*. In addition, our framework is compatible with existing training-based adaptation methods, offering further performance boosts in hybrid scenarios. **Limitations and Future Work.** One of the main limitations of our current design lies in the handling of multiple vision foundation models. While our probabilistic ensemble effectively integrates predictions from different sources, we do not explicitly model feature-level interactions or dynamically weight model contributions. As the number of VFMs increases, naive concatenation or equal-weight fusion may lead to computational overhead or suboptimal alignment. In future work, we plan to explore more sophisticated multi-view feature fusion techniques and dynamic model selection strategies to further enhance performance and scalability.

References

- Azadani, M. N.; Riddell, J.; Sedwards, S.; and Czarnecki, K. 2025. LEO: Boosting Mixture of Vision Encoders for Multimodal Large Language Models. *arXiv preprint arXiv:2501.06986*.
- Bossard, L.; Guillaumin, M.; and Gool, L. V. 2014. Food-101—Mining Discriminative Components with Random Forests. In *Computer Vision – ECCV 2014: 13th European Conference, Zurich, Switzerland, September 6-12, 2014, Proceedings, Part VI* 13, 446–461. Springer.
- Caron, M.; Misra, I.; Mairal, J.; Goyal, P.; Bojanowski, P.; and Joulin, A. 2020. Unsupervised learning of visual features by contrasting cluster assignments. In *Advances in neural information processing systems*, volume 33, 9912–9924.
- Chen, S.; Hong, Z.; Xie, G.-S.; Yang, W.; Peng, Q.; Wang, K.; Zhao, J.; and You, X. 2022. MSDN: Mutually Semantic Distillation Network for Zero-Shot Learning. In *CVPR*, 7612–7621.
- Chen, S.; Hou, W.; Khan, S.; and Khan, F. S. 2024. Progressive semantic-guided vision transformer for zero-shot learning. In *Proceedings of the IEEE/CVF Conference on Computer Vision and Pattern Recognition*, 23964–23974.
- Chen, S.; Hou, W. Q.; Hong, Z.; Ding, X.; Song, Y.; You, X.; Liu, T.; and Zhang, K. 2023. Evolving Semantic Prototype Improves Generative Zero-Shot Learning. In *ICML*, 5542–5557.
- Cimpoi, M.; Maji, S.; Kokkinos, I.; Mohamed, S.; and Vedaldi, A. 2014. Describing Textures in the Wild. In *Proceedings of the IEEE Conference on Computer Vision and Pattern Recognition*, 3606–3613.
- Cuturi, M. 2013. Sinkhorn distances: Lightspeed computation of optimal transport. In *Advances in neural information processing systems*, volume 26.
- Fei-Fei, L.; Fergus, R.; and Perona, P. 2004. Learning Generative Visual Models from Few Training Examples: An Incremental Bayesian Approach Tested on 101 Object Categories. In *Proceedings of the 2004 Conference on Computer Vision and Pattern Recognition Workshop*, 178–178. IEEE.
- Feng, C.-M.; Yu, K.; Liu, Y.; Khan, S.; and Zuo, W. 2023. Diverse data augmentation with diffusions for effective test-time prompt tuning. In *Proceedings of the IEEE/CVF International Conference on Computer Vision*, 2704–2714.
- Fu, Y.; Hospedales, T. M.; Xiang, T.; and Gong, S. 2015. Transductive Multi-view Zero-shot Learning. In *IEEE Transactions on Pattern Analysis and Machine Intelligence (TPAMI)*, volume 37, 2332–2345.
- Guo, Z.; Zhang, R.; Qiu, L.; Ma, X.; Miao, X.; He, X.; and Cui, B. 2023. Calip: Zero-shot enhancement of clip with parameter-free attention. In *Proceedings of the AAAI Conference on Artificial Intelligence*, volume 37, 746–754.
- Han, Z.; Fu, Z.; Chen, S.; and Yang, J. 2021. Contrastive embedding for generalized zero-shot learning. In *Proceedings of the IEEE/CVF conference on computer vision and pattern recognition*, 2371–2381.
- Hou, W.; Chen, S.; Chen, S.; Hong, Z.; Wang, Y.; Feng, X.; Khan, S.; Khan, F. S.; and You, X. 2024. Visual-augmented dynamic semantic prototype for generative zero-shot learning. In *Proceedings of the IEEE/CVF conference on computer vision and pattern recognition*, 23627–23637.
- Hou, W.; Fu, D.; Li, K.; Chen, S.; Fan, H.; and Yang, Y. 2025. ZeroMamba: Exploring visual state space model for zero-shot learning. In *Proceedings of the AAAI Conference on Artificial Intelligence*, volume 39, 3527–3535.
- Hu, X.; Zhang, K.; Xia, L.; Chen, A.; Luo, J.; Sun, Y.; Wang, K.; Qiao, N.; Zeng, X.; Sun, M.; et al. 2024. Reclip: Refine contrastive language image pre-training with source free domain adaptation. In *Proceedings of the IEEE/CVF Winter Conference on Applications of Computer Vision*, 2994–3003.
- Imam, M. F.; Marew, R. F.; Hassan, J.; Fiaz, M.; Aji, A. F.; and Cholakkal, H. 2024. CLIP meets DINO for Tuning Zero-Shot Classifier using Unlabeled Image Collections. *arXiv preprint arXiv:2411.19346*.
- Jia Deng, R. S. L.-J. L. K. L., Wei Dong; and Fei-Fei, L. 2009. Imagenet: A large scale hierarchical image database. In *IEEE Conference on Computer Vision and Pattern Recognition*, 248–255.
- Jianxiong Xiao, K. A. E.-A. O., James Hays; and Torralba, A. 2010. Sun database: Large-scale scene recognition from abbey to zoo. In *IEEE computer society conference on computer vision and pattern recognition*, 3485–3492.
- Jonathan Krause, J. D., Michael Stark; and Fei-Fei, L. 2013. 3d object representations for fine-grained categorization. In *IEEE international conference on computer vision workshops*, 554–561.
- Kalantidis, Y.; Tolias, G.; et al. 2024. Label propagation for zero-shot classification with vision-language models. In *Proceedings of the IEEE/CVF Conference on Computer Vision and Pattern Recognition*, 23209–23218.
- Kar, O. F.; Tonioni, A.; Poklukar, P.; Kulshrestha, A.; Zamir, A.; and Tombari, F. 2024. BRAVE: Broadening the visual encoding of vision-language models. In *European Conference on Computer Vision*, 113–132. Springer.
- Karmanov, A.; Guan, D.; Lu, S.; El Saddik, A.; and Xing, E. 2024. Efficient test-time adaptation of vision-language models. In *Proceedings of the IEEE/CVF Conference on Computer Vision and Pattern Recognition*, 14162–14171.
- Khattak, M. U.; Naeem, M. F.; Naseer, M.; Van Gool, L.; and Tombari, F. 2025. Learning to prompt with text only supervision for vision-language models. In *Proceedings of the AAAI Conference on Artificial Intelligence*, volume 39, 4230–4238.
- Lampert, C. H.; Nickisch, H.; and Harmeling, S. 2009. Learning to Detect Unseen Object Classes by Between-Class Attribute Transfer. In *IEEE Conference on Computer Vision and Pattern Recognition (CVPR)*.
- Li, Y.; Su, Y.; Goodge, A.; Jia, K.; and Xu, X. 2025. Efficient and Context-Aware Label Propagation for Zero-/Few-Shot Training-Free Adaptation of Vision-Language Model. In *The Thirteenth International Conference on Learning Representations*.

- Li, Y.; Zhang, Y.; Wang, C.; Zhong, Z.; Chen, Y.; Chu, R.; Liu, S.; and Jia, J. 2024. Mini-gemini: Mining the potential of multi-modality vision language models. *arXiv preprint arXiv:2403.18814*.
- Liu, M.; Li, F.; Zhang, C.; Wei, Y.; Bai, H.; and Zhao, Y. 2023. Progressive semantic-visual mutual adaption for generalized zero-shot learning. In *Proceedings of the IEEE/CVF conference on computer vision and pattern recognition*, 15337–15346.
- Manli, S.; Weili, N.; De-An, H.; Zhiding, Y.; Tom, G.; Anima, A.; and Chaowei, X. 2022. Test-Time Prompt Tuning for Zero-shot Generalization in Vision-Language Models. In *NeurIPS*.
- Martin, S.; Huang, Y.; Shakeri, F.; Pesquet, J.-C.; and Ben Ayed, I. 2024. Transductive zero-shot and few-shot clip. In *Proceedings of the IEEE/CVF Conference on Computer Vision and Pattern Recognition*, 28816–28826.
- Menon, S.; and Vondrick, C. 2023. Visual Classification via Description from Large Language Models. In *The Eleventh International Conference on Learning Representations*.
- Mirza, M. J.; Karlinsky, L.; Lin, W.; Possegger, H.; Kozinski, M.; Feris, R.; and Bischof, H. 2023. Lafter: Label-free tuning of zero-shot classifier using language and unlabeled image collections. *Advances in Neural Information Processing Systems*, 36: 5765–5777.
- MParkhi, O.; Vedaldi, A.; Zisserman, A.; and Jawahar, C. 2012. Cats and Dogs. In *Proceedings of the 2012 IEEE Conference on Computer Vision and Pattern Recognition*, 3498–3505. IEEE.
- Nilsback, M.-E.; and Zisserman, A. 2008. Automated Flower Classification over a Large Number of Classes. In *Proceedings of the 2008 Sixth Indian Conference on Computer Vision, Graphics & Image Processing*, 722–729. IEEE.
- Novack, Z.; McAuley, J.; Lipton, Z. C.; and Garg, S. 2023. Chils: Zero-shot image classification with hierarchical label sets. In *International Conference on Machine Learning*, 26342–26362. PMLR.
- Oquab, M.; Darcet, T.; Moutakanni, T.; Vo, H.; Szafraniec, M.; Marcou, L.; Haziza, D.; Filliat, D.; Neverova, N.; Mairal, J.; Bojanowski, P.; Jégou, H.; and Caron, M. 2023. DINOv2: Learning Robust Visual Features without Supervision. *arXiv preprint arXiv:2304.07193*.
- Patrick Helber, A. D., Benjamin Bischke; and Borth, D. 2019. Eurosat: A novel dataset and deep learning benchmark for land use and land cover classification. *IEEE Journal of Selected Topics in Applied Earth Observations and Remote Sensing*, 12(7): 2217–2226.
- Pratt, S.; Covert, I.; Liu, R.; and Farhadi, A. 2023. What does a platypus look like? generating customized prompts for zero-shot image classification. In *Proceedings of the IEEE/CVF International Conference on Computer Vision*, 15691–15701.
- Qian, Q.; Xu, Y.; and Hu, J. 2023. Intra-modal proxy learning for zero-shot visual categorization with clip. *Advances in Neural Information Processing Systems*, 36: 25461–25474.
- Radford, A.; Kim, J. W.; Hallacy, C.; Ramesh, A.; Goh, G.; Agarwal, S.; Sastry, G.; Askell, A.; Mishkin, P.; Clark, J.; Krueger, G.; and Sutskever, I. 2021. Learning Transferable Visual Models From Natural Language Supervision. In *International Conference on Machine Learning (ICML)*.
- Roth, K.; Kim, J. M.; Koepke, A.; Vinyals, O.; Schmid, C.; and Akata, Z. 2023. Waffling around for performance: Visual classification with random words and broad concepts. In *Proceedings of the IEEE/CVF International Conference on Computer Vision*, 15746–15757.
- Shazeer, N.; Mirhoseini, A.; Maziarz, K.; Davis, A.; Le, Q.; Hinton, G.; and Dean, J. 2017. Outrageously large neural networks: The sparsely-gated mixture-of-experts layer. In *Proceedings of the International Conference on Learning Representations (ICLR)*.
- Soomro, K.; Zamir, A. R.; and Shah, M. 2012. UCF101: A Dataset of 101 Human Action Classes From Videos in the Wild. *arXiv preprint arXiv:1212.0402*.
- Subhransu Maji, J. K. M. B., Esa Rahtu; and Vedaldi, A. 2013. Fine-grained visual classification of aircraft. *arXiv preprint arXiv:1306.5151*.
- Udandara, V.; Gupta, A.; and Albanie, S. 2023. Sus-x: Training-free name-only transfer of vision-language models. In *Proceedings of the IEEE/CVF International Conference on Computer Vision*, 2725–2736.
- Villani, C.; et al. 2008. *Optimal transport: old and new*, volume 338. Springer.
- Wang, Z.; Hao, Y.; Mu, T.; Li, O.; Wang, S.; and He, X. 2023. Bi-directional distribution alignment for transductive zero-shot learning. In *Proceedings of the IEEE/CVF Conference on Computer Vision and Pattern Recognition*, 19893–19902.
- Zanella, M.; Gérin, B.; and Ayed, I. 2024. Boosting vision-language models with transduction. *Advances in Neural Information Processing Systems*, 37: 62223–62256.
- Zhang, J.; Wei, Q.; Liu, F.; and Feng, L. 2024a. Candidate Pseudolabel Learning: Enhancing Vision-Language Models by Prompt Tuning with Unlabeled Data. In *Forty-First International Conference on Machine Learning*.
- Zhang, R.; Hu, X.; Li, B.; Huang, S.; Deng, H.; Qiao, Y.; Gao, P.; and Li, H. 2023. Prompt, generate, then cache: Cascade of foundation models makes strong few-shot learners. In *Proceedings of the IEEE/CVF conference on computer vision and pattern recognition*, 15211–15222.
- Zhang, X.; and Tan, R. T. 2025. Mamba as a Bridge: Where Vision Foundation Models Meet Vision Language Models for Domain-Generalized Semantic Segmentation. In *Proceedings of the IEEE/CVF Conference on Computer Vision and Pattern Recognition*.
- Zhang, Y.; Zhu, W.; Tang, H.; Ma, Z.; Zhou, K.; and Zhang, L. 2024b. Dual memory networks: A versatile adaptation approach for vision-language models. In *Proceedings of the IEEE/CVF conference on computer vision and pattern recognition*, 28718–28728.

Zhou, K.; Yang, J.; Loy, C. C.; and Liu, Z. 2022a. Conditional prompt learning for vision-language models. In *Proceedings of the IEEE/CVF conference on computer vision and pattern recognition*, 16816–16825.

Zhou, K.; Yang, J.; Loy, C. C.; and Liu, Z. 2022b. Learning to Prompt for Vision-Language Models. *International Journal of Computer Vision (IJCV)*.

Zhou, Y.; Ren, J.; Li, F.; Zabih, R.; and Lim, S. N. 2023. Test-time distribution normalization for contrastively learned visual-language models. *Advances in Neural Information Processing Systems*, 36: 47105–47123.